

## Optical Necklace States in Anderson Localized 1D Systems

Jacopo Bertolotti, Stefano Gottardo, and Diederik S. Wiersma

*European Laboratory for Nonlinear Spectroscopy and INFM, 50019 Sesto Fiorentino (Florence), Italy*

Mher Ghulinyan and Lorenzo Pavesi

*INFM and Department of Physics, University of Trento, I-38050 Povo (Trento), Italy*

(Received 8 November 2004; published 22 March 2005)

We report on the observation of nonlocalized modes or necklace states of light waves in disordered systems in the Anderson localized regime. The samples consist of positional-disordered binary multilayer systems. Anderson localized modes manifest themselves as narrow high-transmission peaks in the transmission spectrum, whereas the average of the logarithm of the transmission coefficient decreases linearly with thickness. Optical necklace states are observed as modes with a characteristic multi-resonance time response and relatively fast decay time.

DOI: 10.1103/PhysRevLett.94.113903

PACS numbers: 42.25.Dd, 05.40.Fb, 42.25.Hz, 42.55.Zz

Light waves in disordered materials are subject to a multiple scattering process in which interference effects can play an important role. This leads to interesting optical phenomena [1] of which the most surprising is that of Anderson localization of light [2]. Anderson localization was originally discovered for electron transport, where the diffusion of electrons was found to disappear upon increasing the disorder inside a conductor [3–5]. It was found that the interference between multiply scattered Schrödinger waves leads to localized eigenfunctions that decay exponentially [6]. Being a pure interference phenomenon, Anderson localization is expected to occur also for classical waves such as electromagnetic radiation [2]. The observation of this extraordinary effect in three dimensional disordered optical systems requires very strong scattering that can be achieved only in selected materials [7]. For lower dimensional systems, however, the situation is different. In one and two dimensional disordered systems, localization can always be reached for a sufficiently large sample size [8]. In particular, one dimensional (1D) optical systems have the advantage that samples can be fabricated with complete control over the type and degree of disorder, using molecular beam epitaxy [9], rf-magnetron sputtering [10], or electrochemical etching [11]. The field distribution can be calculated exactly and a direct link exists between light and electron transport described by a 1D tight-binding model.

The transmission spectra of localized 1D systems exhibit many randomly distributed high-transmission peaks. These high-transmission peaks originate from resonances created inside the sample by localized modes [12] and result in big fluctuations in the transmission coefficient  $T$  [1,13]. The localized modes decay exponentially and, as a consequence, the ensemble average of  $\ln T(\lambda)$  over many realizations of the disorder decays linearly with the sample thickness  $L$  [14]. A pioneering experiment to investigate 1D localization was performed by Daozhong *et al.* [15] on thin binary multilayer systems.

Not all states in 1D disordered systems are Anderson localized. Pendry [16] and Tartakovskii [17] predicted that even in 1D localized systems nonlocalized modes exist that extend over the sample via multiple resonances [18]. These nonlocalized modes, called necklace states, have a transmission coefficient close to 1 and become extremely rare upon increasing the sample thickness. Nevertheless, they dominate the average transmission coefficient, even at large thickness.

In this Letter we report on the observation of both localized and necklace modes in disordered one-dimensional systems. The samples consist of disordered multilayer structures obtained via controlled electrochemical etching of silicon. We observe characteristic high-transmission peaks due to resonances inside the sample and determine the localization length from the thickness dependence of the transmission. We demonstrate that one can distinguish between single resonance localized modes and multi-resonance nonlocalized modes in time-resolved transmission experiments. The observed number of necklace states is consistent with theoretical predictions.

We studied samples composed of  $N$  dielectric layers of two types (called  $A$  and  $B$ ) with different refractive indices  $n_A$  and  $n_B$  and with thicknesses  $d_A$  and  $d_B$  (respectively, 258.6 and 176.0 nm). The refractive indices were taken such that  $4n_A d_A = 4n_B d_B = \lambda_0 = 1500$  nm. The disorder was introduced by giving each layer a 50% probability to be of type  $A$  or  $B$ . The samples were realized in porous silicon. We have grown nine disordered samples of various thicknesses in the range from 60 to 350 layers (i.e., with physical thickness between 13 and 76  $\mu\text{m}$ ), starting from (100)-oriented heavily doped  $p$ -type silicon. The etchant was prepared mixing a 30% volumetric fraction of aqueous HF (48 wt %) with ethanol. The applied current density defined the porosity of the layers. We used 50 mA/cm<sup>2</sup> for the high porosity layers  $A$  (porosity 75%, corresponding to refractive index  $n_A = 1.45$ ) and 7 mA/cm<sup>2</sup> for the low porosity layers  $B$  (porosity 49%, corresponding to

$n_B = 2.13$ ). The pores are cylindrically shaped and oriented along the growth direction with diameter between 40–50 nm. The pore diameter determines the porosity and is constant over each layer. The change of pore diameter between two layers of different porosity gives rise to minor scattering losses. The total loss, given by scattering losses and absorption, is expressed by the extinction coefficient which for our samples is  $\kappa_e = (1.0 \pm 0.2) \times 10^2 \text{ cm}^{-1}$  [11]. This loss lowers the transmission coefficient somewhat but does not change the characteristics of the light transport in our samples [19]. The physical thickness  $d$  of the layers was controlled by adjusting the duration of the etch times. The structures were made freestanding by applying a high current pulse at the end of the growth process.

Transmission spectra of the samples were measured in the 1–2  $\mu\text{m}$  wavelength range using a tungsten Halogen lamp focused to a 300  $\mu\text{m}$  diameter spot on the sample. The spectra were recorded with 1 nm wavelength resolution using a monochromator coupled to an infrared photo-sensitive resistor. In Fig. 1 examples of measured transmission spectra are shown for three values of the

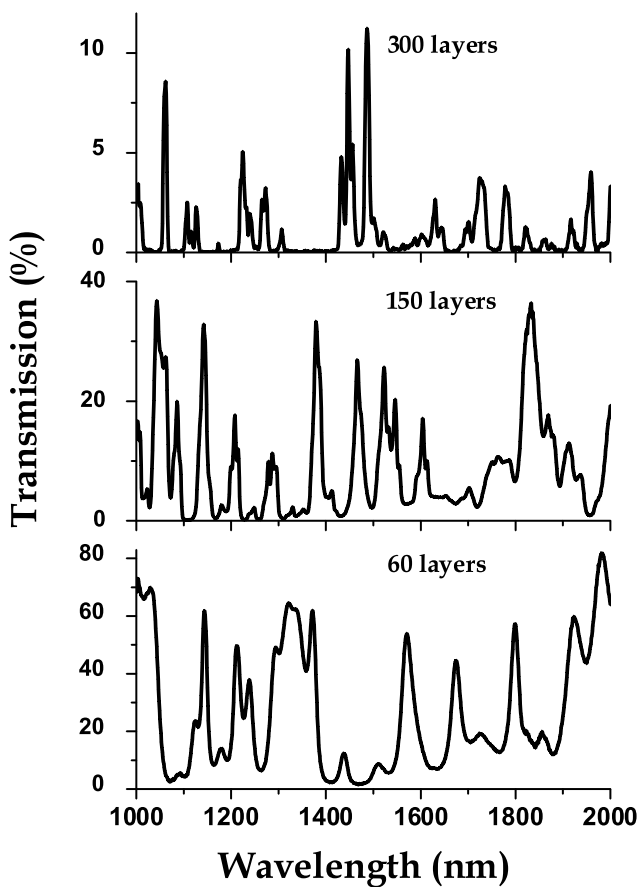


FIG. 1. Measured transmission spectra for three values of the sample thickness  $L$ . The spectra contain narrow high-transmission peaks that, on average, become narrower upon increasing  $L$ .

sample thickness. The high-transmission peaks are typical for a localized system and are due to internal resonances inside the sample. We can see that upon increasing sample thickness, on average, the spectral width of the peaks narrows, as is expected for localized modes. The apparent lowering of the transmission maxima at larger sample thickness is an artifact due to the limited spectral resolution of the monochromator and the minor losses in the sample.

The localized modes decay exponentially over a typical length scale called the localization length  $\xi$ . The transmission coefficient is therefore related to the localization length via [13]:  $\langle \ln T \rangle = -L/\xi$ , where the brackets denote an average over many realizations of the disorder. These ensemble averages are not easily accessible in experiments because they would involve performing transmission measurements on a very large number of samples. The problem can be circumvented, however, assuming ergodicity and thus taking the average over  $\lambda$  on a limited set of samples.

To determine the localization length in our samples, we have calculated the wavelength average of the logarithm of the transmission coefficient for each measured spectrum. The results are plotted in Fig. 2. The dashed line is a linear fit to the data. To determine the localization length from the data, one must take the total loss of the system into account. For nonzero loss, the average of the logarithm of  $T$  is given by  $\langle \ln T \rangle = -L/(\xi + \kappa_e^{-1})$ . For the localization length in our samples we obtain in this way  $\xi = 14.9 \pm 2.4 \mu\text{m}$ . This confirms that the physical sample thickness  $L$  exceeds the localization length and hence that our samples are in the Anderson localized regime.

This opens up the possibility to look for the occurrence of nonlocalized or necklace states in our samples. Necklace states arise when more than one resonance exists in the sample at very similar frequency. This leads to a mode that is extended over the entire sample via (nearly evenly

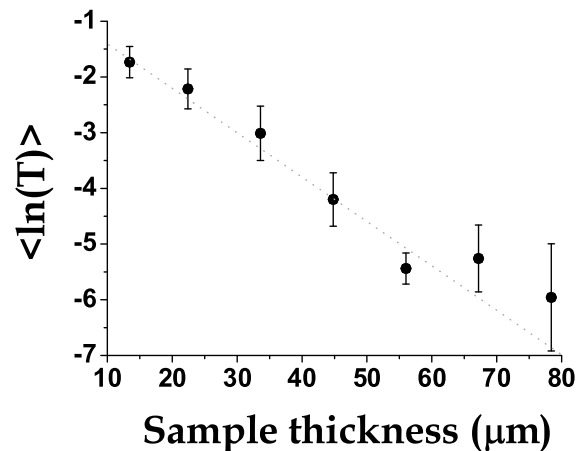


FIG. 2. Spectral average of the logarithm of the measured transmission versus sample thickness. The error bars are obtained by repeating the measurement in various spots on the sample and therefore reflect lateral sample inhomogeneities.

spaced) multiple resonances. Upon increasing the sample thickness, the typical number of resonances increases, and hence these modes become exceedingly rare. Pendry [16] showed that, although being rare, these nonlocalized modes dominate the total transmission since they lead to broad peaks in the transmission spectrum with a transmission coefficient close to 1. The necklace transmission peaks are non-Lorentzian. Transmission peaks due to localized modes, on the other hand, are spectrally narrow and have a Lorentzian line shape.

To identify necklace modes in practice, standard wavelength-resolved transmission experiments are not ideal. The transmission peaks become spectrally very narrow for large  $L$ , which makes it difficult to determine their width and shape accurately. A clear signature of necklace states can be expected, however, in time-resolved experiments. The Lorentzian line shape associated to a localized mode will give rise to an asymmetric time response with an exponentially decaying tail. This is the typical time re-

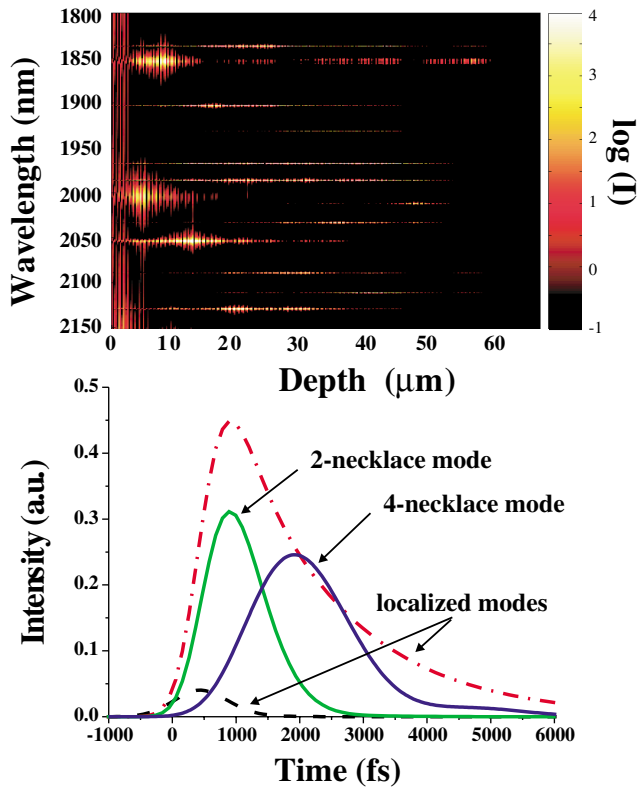


FIG. 3 (color). Top panel: calculated intensity distribution inside the sample. The internal resonances are localized modes. In rare occasions multiple resonances couple and lead to extended necklace modes. A 4-resonance necklace state can be observed around  $\lambda = 1855$  nm. Bottom panel: Transfer-matrix calculation of the transmission of a short laser pulse. Dashed curves: localized modes with high (red) and low (black)  $Q$  factor. Solid lines: necklace states, with two (green), respectively, four (blue) resonances. The refractive indices and pulse duration were taken equal to the experimental values.

sponse of a single resonance, and its quality factor ( $Q$  factor) will determine the delay of the pulse and exponential decay time. The time response of a necklace state will be different since the mode consists of several coupled resonances. This leads to a time response that is more symmetric and delayed, with a delay time determined by the number of resonances. The decay time of a necklace state is relatively fast since it is determined by the inverse of its spectral width.

Figure 3 illustrates the typical behavior for single- and multiple-resonance propagation, as calculated for a one-dimensional disordered system using a standard transfer-matrix formalism [11]. The top panel shows the distribution of the intensity inside the sample in a certain wavelength range, whereas the bottom panel shows the time response of the system in four cases: two localized modes (single resonances) and two examples of necklace states (multiple-resonance modes). The red and black dashed curves correspond to localized modes with high, respectively, low  $Q$  factor. One can see that in the case of a localized mode the pulse is asymmetric with an exponentially decaying tail and that a high transmission is associ-

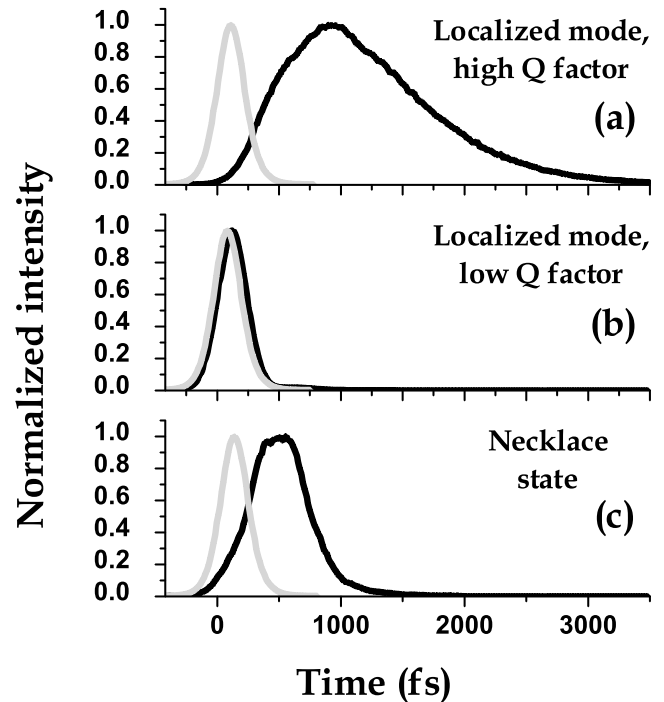


FIG. 4. Time-resolved transmission data. In (a) and (b) a localized mode is probed, with high, respectively, low  $Q$  factor. In (c) a nearly symmetric pulse shape is observed that exhibits a fast decay time and a relatively large delay, typical for a multiple-resonance necklace state. Sample thickness: 250 layers. Gray curves: instrumental response (cross correlation between probe and gate), corrected for the trivial delay introduced by the effective refractive index  $n_{\text{eff}} = (d_A n_A + d_B n_B)/(d_A + d_B)$  of the sample.

ated with a slow decay (strong confinement, high  $Q$  factor). The decay time and pulse delay are directly related in this case. The multiresonance necklace states, on the other hand, result in a more symmetric pulse, of which the delay is determined by the number of resonances (green and blue solid lines). The decay time is relatively fast in this case. The 4-resonance necklace state can be seen in the top panel of Fig. 3 at about  $\lambda = 1855$  nm. The mode consists of four maxima that are nearly evenly distributed in the sample.

To identify possible necklace states experimentally, we performed time-resolved transmission measurements using an optical-gating technique. The probe pulse was generated by an optical parametric oscillator (tunable between 1300 and 1600 nm with an average power of 100 mW) pumped by a mode-locked Ti:sapphire laser with central wavelength at 810 nm (pulse duration 130 fs, average power 2.0 W, and repetition rate 82 MHz). The gate signal was obtained from the residual Ti:sapphire beam (average power 450 mW). The sum frequency generation between the transmitted pulse and the gate signal was obtained using a beta barium borate nonlinear crystal (0.3 mm thick). Noise was suppressed with a standard lock-in technique. In Fig. 4, three examples of such measurements are shown, corresponding to three typical cases. The time response of localized modes with high, respectively, low  $Q$  factor is given in 4(a) and 4(b). One can see that the high  $Q$  factor localized mode gives rise to the characteristic asymmetric response of a single resonance with an exponentially decaying tail. In 4(c) a measurement is shown exhibiting a nearly symmetric pulse with fast decay time and relatively long delay. This is the expected time response of a multiple-resonance nonlocalized mode or necklace state [14,16]. The observed necklace state is most likely of second order.

In our set of samples we observed two modes out of 14 that exhibited the characteristic time response of a necklace state. The probability  $P_n$  of the occurrence of a necklace mode of order  $n$  in a spectral interval  $S$  containing  $M$  modes can be estimated as follows. A necklace state of order  $n$  occurs when  $n$  resonances are superimposed in wavelength within their width  $\Delta K_n$ . We therefore can write

$$P_n \cong \left( \Delta K_n \frac{M}{S} \right)^{n-1}. \quad (1)$$

While both  $S$  and  $M$  can be measured directly, the width  $\Delta K_n$  cannot, since it depends on  $n$ . A very good estimate of  $\Delta K_1$  can, however, be made by measuring the width of the narrowest peak in the spectrum. Assuming that the multiple resonances of the necklace mode are nearly equally distributed over the thickness of the sample one can relate  $\Delta K_n$  to  $\Delta K_1$  by [14]:

$$\Delta K_n = e^{L(n-1)/[2\xi(n+1)]} \Delta K_1. \quad (2)$$

We can thus write the total probability that a given peak is

actually a necklace state as

$$P_{\text{tot}} = \sum_{n=2}^{\infty} \left( e^{L(n-1)/[2\xi(n+1)]} \Delta K_1 \frac{M}{S} \right)^{n-1}. \quad (3)$$

In our case, the above formula gives  $P_{\text{tot}} = 0.2$  for the sample of 250 layers, which means that one can expect that a fraction of 0.2 of the modes in that sample is a necklace state.

We wish to thank Valentin Freilikher, Claudio Oton, and Luca dal Negro for discussions, and especially John Pendry for discussions and his patience in explaining the theory of necklace states. This work was financially supported by the INFN projects RANDS and Photonic and by Miur Cofin 2002 and FIRB ‘‘Sistemi Miniaturizzati per Elettronica e Fotonica’’ and ‘‘Molecular and Organic/Inorganic Hybrid Nanostructures for Photonics.’’

- 
- [1] See, e.g., Ping Sheng, *Introduction to Wave Scattering, Localization, and Mesoscopic Phenomena* (Academic Press, New York, 1995).
  - [2] S. John, Phys. Rev. Lett. **53**, 2169 (1984); P. W. Anderson, Philos. Mag. B **52**, 505 (1985); K. Arya, Z. B. Su, and J. L. Birman, Phys. Rev. Lett. **57**, 2725 (1986); A. Lagendijk, M. P. v. Albada, and M. P. v.d. Mark, Physica (Amsterdam) **140A**, 183 (1986).
  - [3] P. W. Anderson, Phys. Rev. **109**, 1492 (1958).
  - [4] E. Abrahams *et al.*, Phys. Rev. Lett. **42**, 673 (1979).
  - [5] P. A. Lee and T. V. Ramakrishnan, Rev. Mod. Phys. **57**, 287 (1985).
  - [6] N. F. Mott, *Metal-Insulator Transition* (Taylor & Francis, London, 1974).
  - [7] R. Dalichaouch *et al.*, Nature (London) **354**, 53 (1991); D. S. Wiersma *et al.*, Nature (London) **390**, 671 (1997); A. A. Chabanov and A. Z. Genack, Phys. Rev. Lett. **87**, 233903 (2001).
  - [8] N. F. Mott and W. D. Twose, Adv. Phys. **10**, 107 (1961); D. J. Thouless, Phys. Rev. Lett. **39**, 1167 (1977).
  - [9] R. P. Stanley *et al.*, Appl. Phys. Lett. **65**, 2093 (1994).
  - [10] L. dal Negro *et al.*, Appl. Phys. Lett. **84**, 5186 (2004).
  - [11] L. dal Negro *et al.*, Phys. Rev. Lett. **90**, 055501 (2003); M. Ghulinyan *et al.*, J. Appl. Phys. **93**, 9724 (2003).
  - [12] M. Ya. Azbel, Phys. Rev. B **28**, 4106 (1983).
  - [13] J. A. Sánchez-Gil and V. Freilikher, Phys. Rev. B **68**, 075103 (2003); K. Yu. Bliokh, Yu. P. Bliokh, and V. Freilikher, J. Opt. Soc. Am. B **21**, 113 (2004).
  - [14] J. B. Pendry, Adv. Phys. **43**, 461 (1994).
  - [15] Z. Daozhong *et al.*, Phys. Rev. B **50**, 9810 (1994).
  - [16] J. B. Pendry, J. Phys. C **20**, 733 (1987).
  - [17] A. V. Tartakovskii *et al.*, Sov. Phys. Semicond. **21**, 370 (1987).
  - [18] See also M. E. Raikh and I. M. Ruzin, in *Mesoscopic Phenomena in Solids*, edited by B. L. Altshuler, P. A. Lee, and R. A. Webb (North-Holland, Amsterdam, 1991).
  - [19] The extinction length  $\kappa_e^{-1} = 0.1$  mm is almost an order of magnitude longer than the localization length of 14.9  $\mu\text{m}$ .